SAND2016-7079C

Exceptional service in the national interest

Sandia National Laboratories

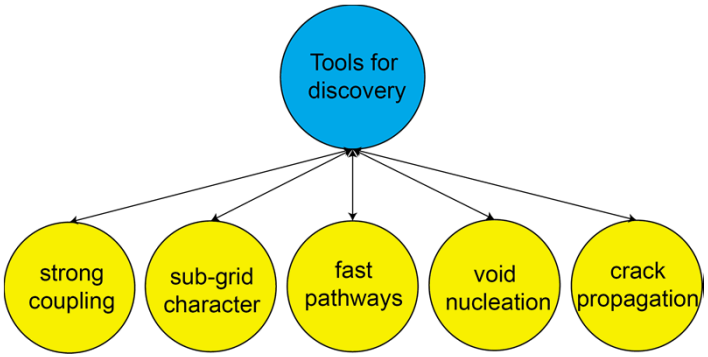

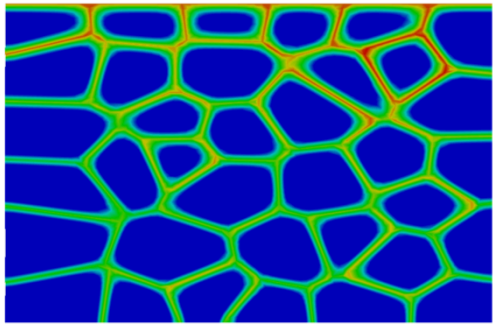

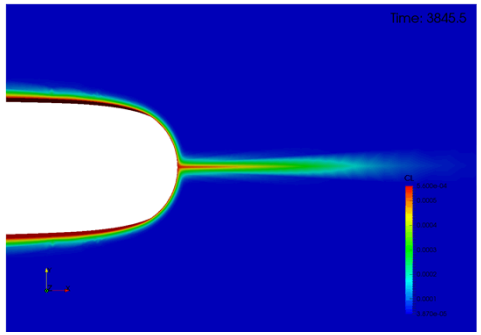

Simulating hydrogen embrittlement and fast pathways for diffusion

J. Foulk III, J. Ostien, A. Mota, Steve Sun, Guy Bergel, Gabriel de Frias

Collaborators: Bill Wolfer, C. San Marchi, B. Somerday

October 27, 2016

U.S. DEPARTMENT OF ENERGY

NNSA National Nuclear Security Administration

Sandia National Laboratories is a multi-program laboratory managed and operated by Sandia Corporation, a wholly owned subsidiary of Lockheed Martin Corporation, for the U.S. Department of Energy's National Nuclear Security Administration under contract DE-AC04-94AL85000. SAND NO. 2011-XXXXP

Tools for discovery and prediction

Sandia National Laboratories

- Motivated through observation
- Strong chemo-mechanical coupling
- Capture sub-grid processes through a surface approach
- Explore fast pathways for diffusion at structural and microstructural scales
- Develop models for H/T/He embrittlement w/focus on void nucleation
- Demonstrate crack initiation and propagation via the SFC

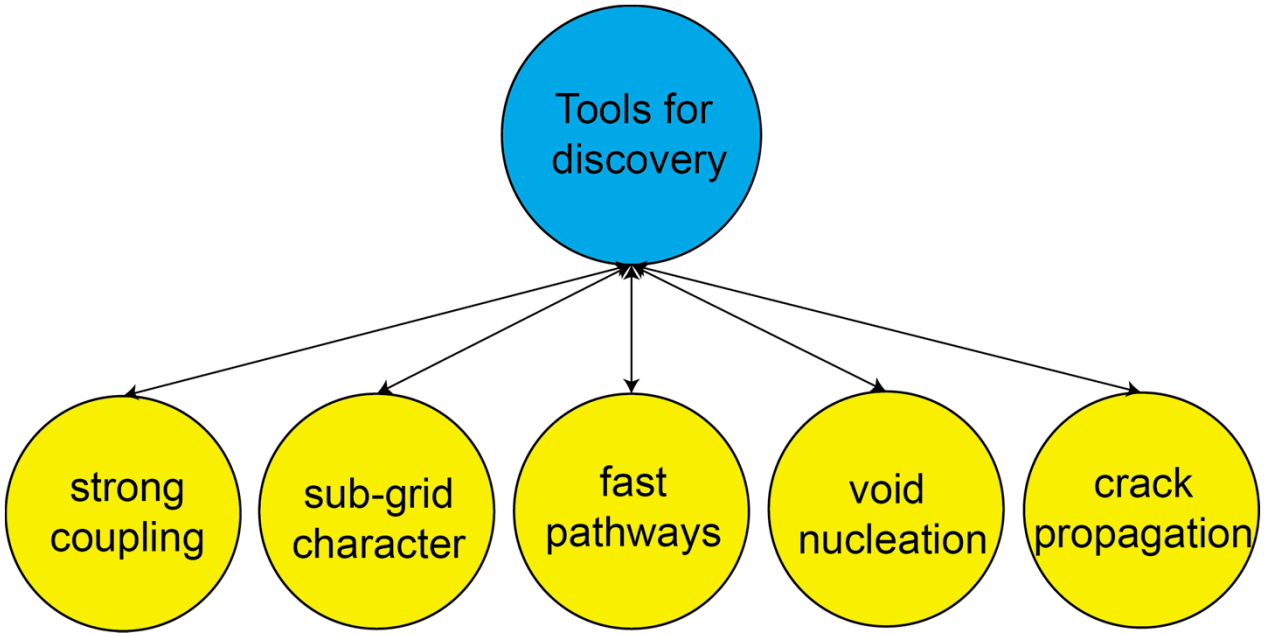

Initial studies in 21Cr-6Ni-9Mn SS

- Compact tension specimens, B ~ 13 mm; W ~ 26 mm
- Constant pressure of gaseous hydrogen: 103 MPa
- "Loading rates" ~ 0.6 - 10 MPa $m^{1/2}$ per minute

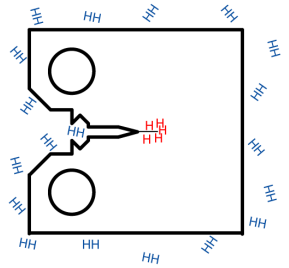

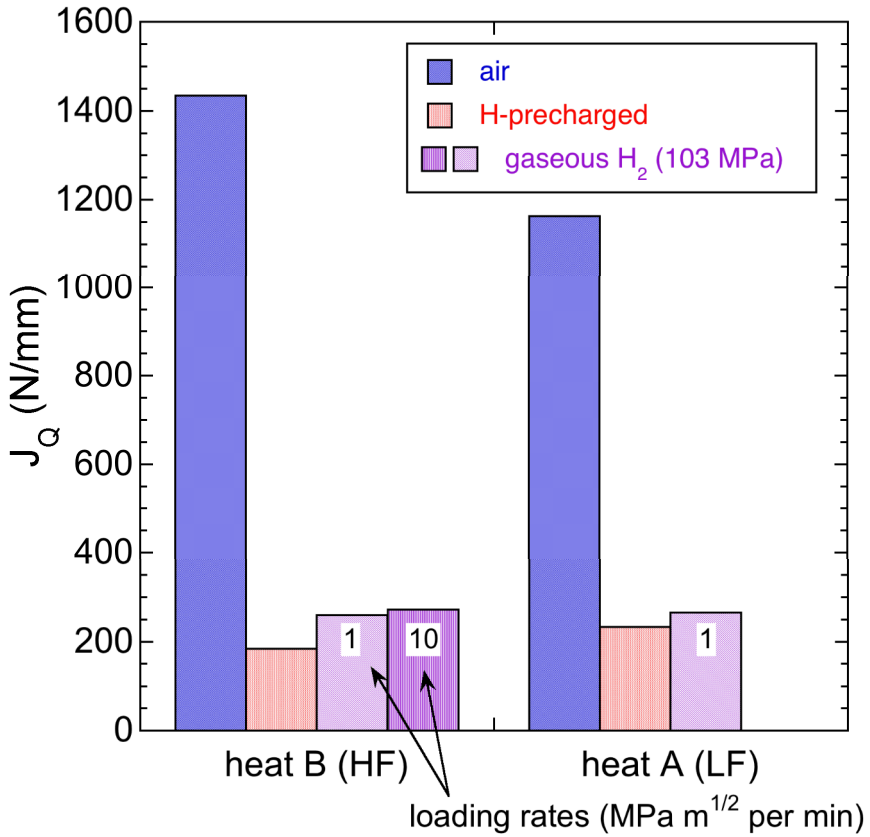

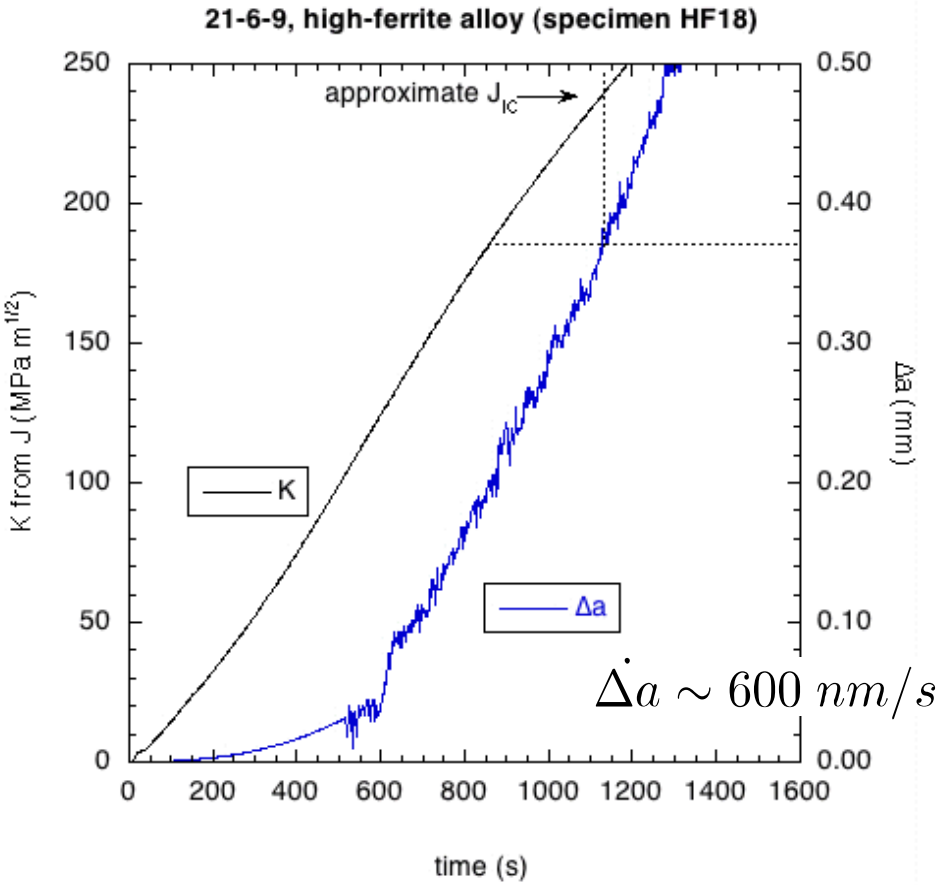

Note: 220 MPa $m^{1/2}$ = 224 kJ/m^2 (N/mm)

(C. San Marchi, SNL)

Aging of stainless steels in H isotopes

- Fracture toughness degrades with increasing helium concentrations
- Both tritium and helium are requisite for degradation
- Transition from void evolution to fracture along twin and grain boundaries

Morgan and Tosten, Tritium and decay helium effects on the fracture toughness, International Conference on Hydrogen (1994)

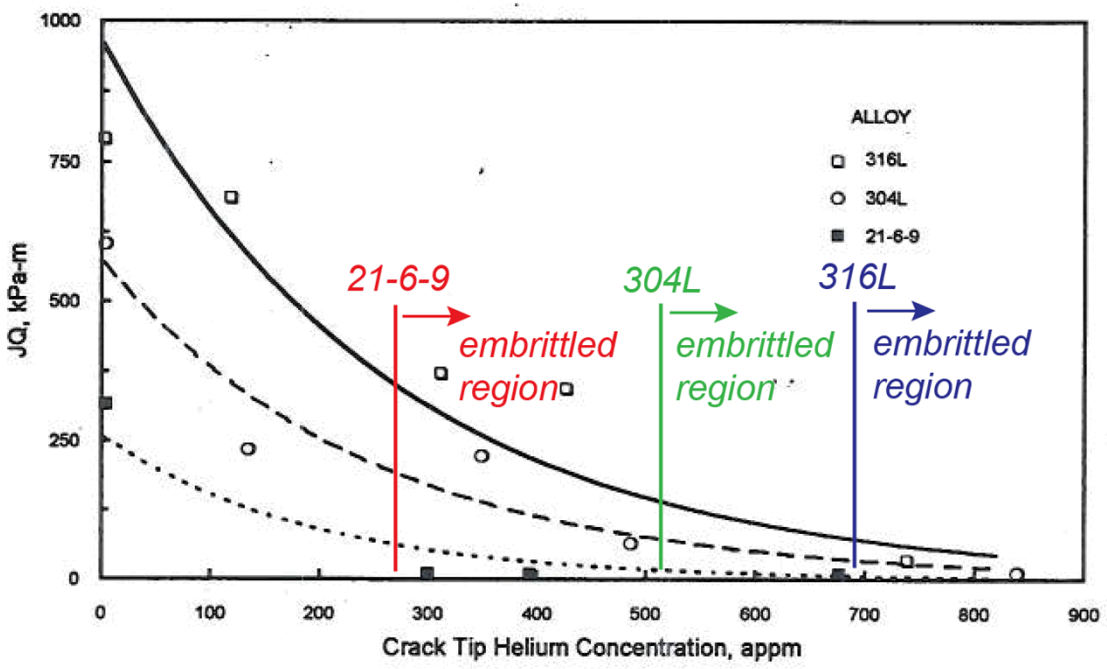

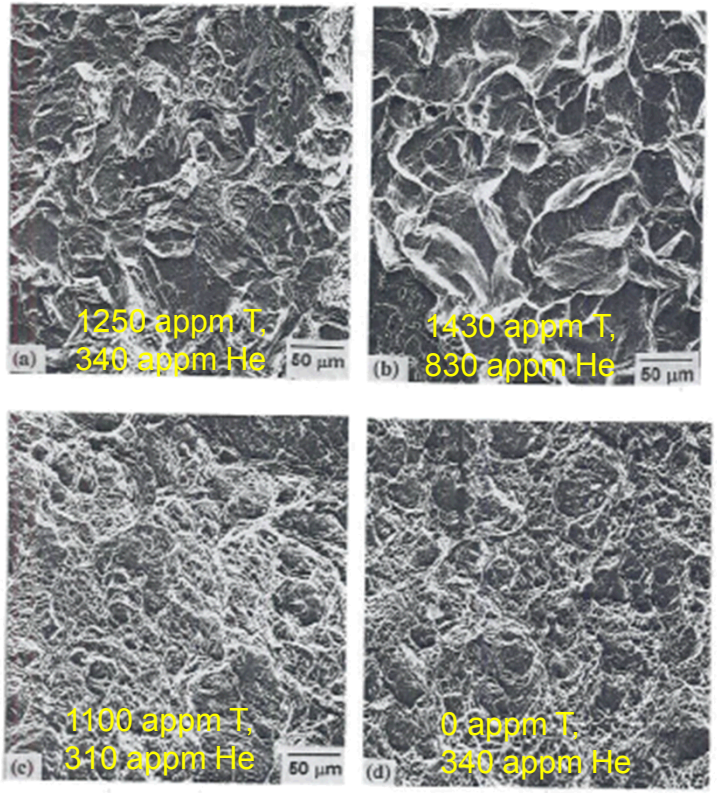

Figure 4 - Fracture Modes In Tritium-Exposed-And-Aged Stainless Steels: (a) Type 304L, 1250 Tritium, 340 appm He; (b) Type 304L, 1430 Appm Tritium, 830 appm He; (c) Type 316L Steel 1100 appm Tritium 310 appm He; (d) Type 304L, Tritium Degassed, ~ 0 appm T, 340 appm He.

Finite deformation diffusion of H

This path heavily leverages Sofronis/McMeeking (1989)* and Krom (1998). Recent work by Leo and Anand (2013).

Transport of hydrogen in the current configuration

$$D^*\dot{c}_l + C^*\mathrm{div}\boldsymbol{v} - \nabla_{\boldsymbol{x}}\cdot\boldsymbol{d}_l\nabla_{\boldsymbol{x}}c_l - \nabla_{\boldsymbol{x}}\cdot\frac{c_l}{J}\boldsymbol{d}_l\nabla_{\boldsymbol{x}}J + \nabla_{\boldsymbol{x}}\cdot\frac{c_l V_H}{RT}\boldsymbol{d}_l\nabla_{\boldsymbol{x}}\tau_h + \frac{\theta_l}{J}\frac{\partial N_T}{\partial\epsilon_p}\dot{\epsilon}_p - \frac{\theta_t N_T}{J^2}\dot{J} = 0$$

Transport of hydrogen in the reference configuration (push back)

$$D^*\dot{C}_L - \nabla_{\boldsymbol{X}}\cdot d_l\boldsymbol{C}^{-1}\nabla_{\boldsymbol{X}}C_L + \nabla_{\boldsymbol{X}}\cdot\frac{d_l V_H}{RT}\boldsymbol{C}^{-1}\nabla_{\boldsymbol{X}}\tau_h C_L + \theta_T\frac{dN_T}{d\epsilon_p}\dot{\epsilon}_p$$

transient term

diffusion term

advection term from pressure

source term from trapping

Deformation-dependent diffusivity $\boldsymbol{D}_L = \boldsymbol{F}^{-1}\boldsymbol{d}_l\boldsymbol{F}^{-T} = d_l\boldsymbol{C}^{-1}$

Capture sub-grid processes for R(a)

Goal: Capture sub-grid processes through methods that regularize the jump

$$\boldsymbol{F} = \boldsymbol{F}^{\parallel}\,\boldsymbol{F}^{\perp}$$

$$\boldsymbol{F}^{\parallel} = \boldsymbol{g}_i \otimes \boldsymbol{G}^i$$

$$\boldsymbol{F}^{\perp} = \boldsymbol{I} + \frac{[\![\boldsymbol{\Phi}]\!]}{h} \otimes \boldsymbol{N}$$

$$\boldsymbol{F} = \boldsymbol{F}^{\parallel} + \frac{[\![\boldsymbol{\varphi}]\!]}{h} \otimes \boldsymbol{N}$$

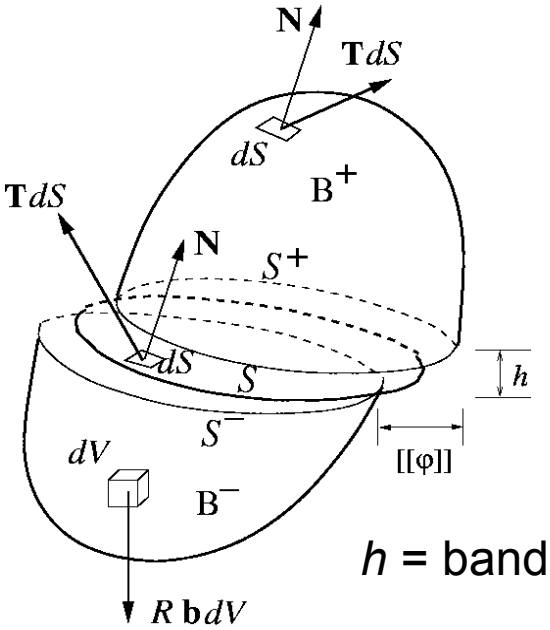

h = band thickness

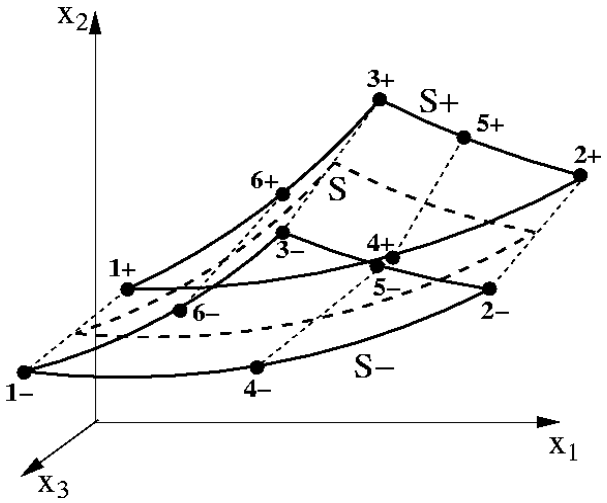

Akin to "cohesive" element

- Finite-deformation kinematics
- Simulation of strain localization
- No additional constitutive assumptions

Yang, Mota and Ortiz (IJNME, 2005), Armero and Garikipati (IJSS, 1996)

Extend sub-grid model for multiphysics

Sandia National Laboratories

Fox and Simo (1990), Callari, Armero, Abati (2010)

redefine space

$$\boldsymbol{X} = \boldsymbol{\Phi}(\xi^1, \xi^2, \xi^3) = \bar{\boldsymbol{\Phi}}(\xi^1, \xi^2) + \boldsymbol{N}(\xi^1, \xi^2)\xi^3 \qquad \boldsymbol{G}_i = \boldsymbol{\Phi}_{,i} = \frac{\partial \boldsymbol{X}}{\partial \xi^i}$$

include jump in C

$$C(\boldsymbol{X}) = \bar{C}(\boldsymbol{\phi}[\xi^1, \xi^2]) + \frac{[\![C]\!](\boldsymbol{\phi}[\xi^1, \xi^2])}{h}\xi^3 \qquad \nabla_{\boldsymbol{X}} C = (\nabla \boldsymbol{\Phi})^{-T} \frac{\partial C}{\partial \xi^i}$$

Finite element implementation is straightforward

$$\nabla_{\boldsymbol{X}} C\big|_{\xi^3=0} = [B] \begin{bmatrix} \{C\}^+ \\ \{C\}^- \end{bmatrix} = \begin{bmatrix} [B]^+ & [B]^- \end{bmatrix} \begin{bmatrix} \{C\}^+ \\ \{C\}^- \end{bmatrix}$$

$$B^{\pm}_{ia} = \begin{bmatrix} G^1_i & G^2_i & G^3_i \end{bmatrix} \cdot \begin{bmatrix} \frac{1}{2}\frac{\partial N_a}{\partial \xi^1} & \frac{1}{2}\frac{\partial N_a}{\partial \xi^2} & \pm\frac{1}{h}N_a \end{bmatrix}$$

i = # dimensions, *a* = # nodes

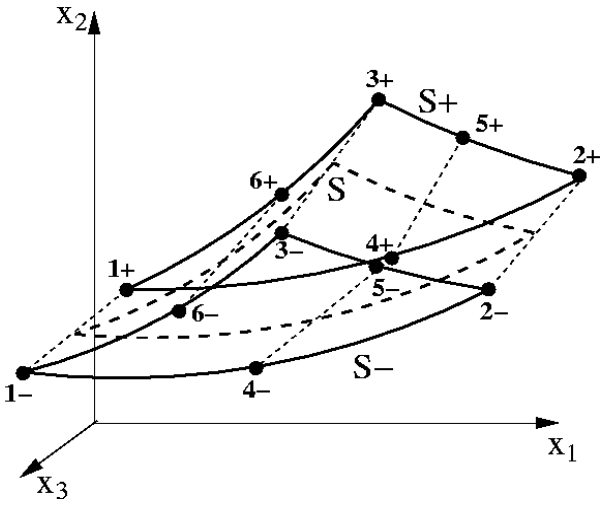

Given this gradient operator, we can use the same PDE for finite-deformation diffusion

$$D^* \dot{C}_L - \nabla_{\boldsymbol{X}} \cdot d_l \boldsymbol{C}^{-1} \nabla_{\boldsymbol{X}} C_L + \nabla_{\boldsymbol{X}} \cdot \frac{d_l V_H}{RT} \boldsymbol{C}^{-1} \nabla_{\boldsymbol{X}} \tau_h C_L + \theta_T \frac{dN_T}{d\epsilon_p} \dot{\epsilon}_p$$

Simple channel w/fast pathway

Implementation of fast pathway (no deformation):

$$\int_{\mathcal{B}^G} \nabla_{\boldsymbol{X}} v D_L(\boldsymbol{X}) \nabla_{\boldsymbol{X}} C \, dV \approx h \sum_{j=1}^{N_{\text{int}}^M} \overline{W}(\xi_j^1, \xi_j^2) \begin{bmatrix} v_a^+(\xi_j^1, \xi_j^2) & v_a^-(\xi_j^1, \xi_j^2) \end{bmatrix} \begin{bmatrix} \vec{B}^+(\xi_j^1, \xi_j^2) \\ \vec{B}^-(\xi_j^1, \xi_j^2) \end{bmatrix} D_L(\boldsymbol{X}) \begin{bmatrix} \vec{B}^+(\xi_j^1, \xi_j^2) & \vec{B}^-(\xi_j^1, \xi_j^2) \end{bmatrix} \begin{bmatrix} C_a^+ \\ C_a^- \end{bmatrix}$$

Surface fast pathway

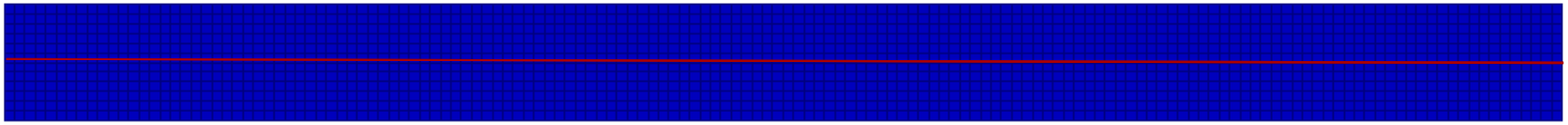

Channel fast pathway

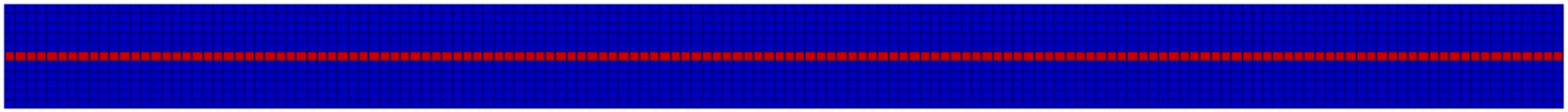

Surface fast pathway, $10^5 D_0$

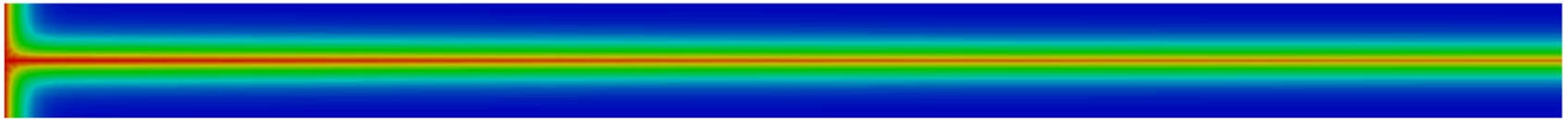

Channel fast pathway, , $10^5 D_0$

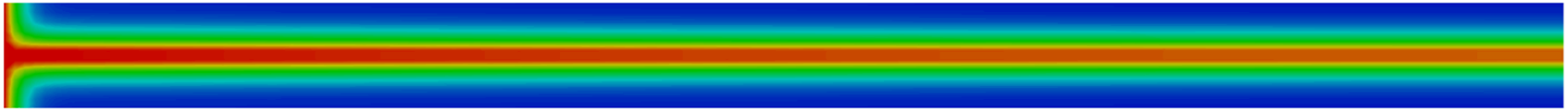

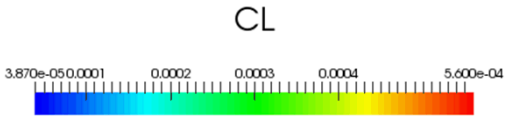

Polycrystals with fast pathway

Grain interface diffusion coupled with mechanical loading:

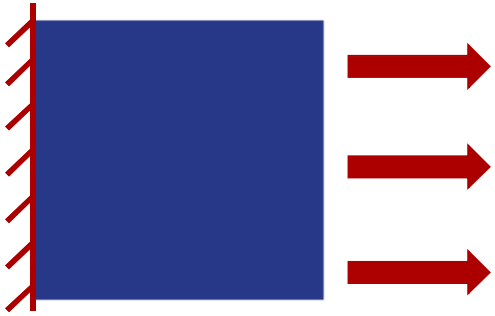

- Stretched in horizontal direction
- Fast pathway = $10^5 D_0$
- Horizontal diffusion
- Vertical diffusion

$$\boldsymbol{D}_L = \boldsymbol{F}^{-1}\boldsymbol{d}_l\boldsymbol{F}^{-T} = d_l\boldsymbol{C}^{-1}$$

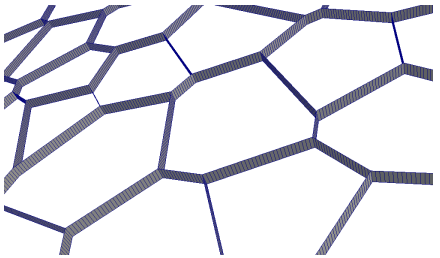

Horizontal diffusion

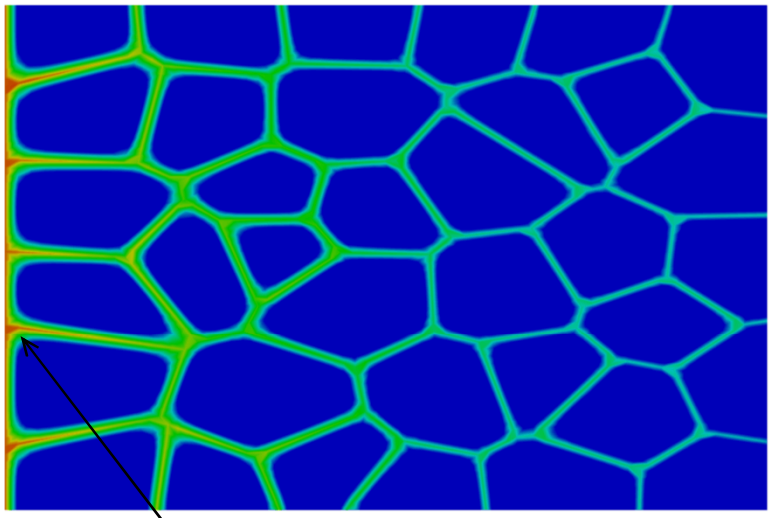

Diffusion slows down due to increasing length.

Vertical diffusion

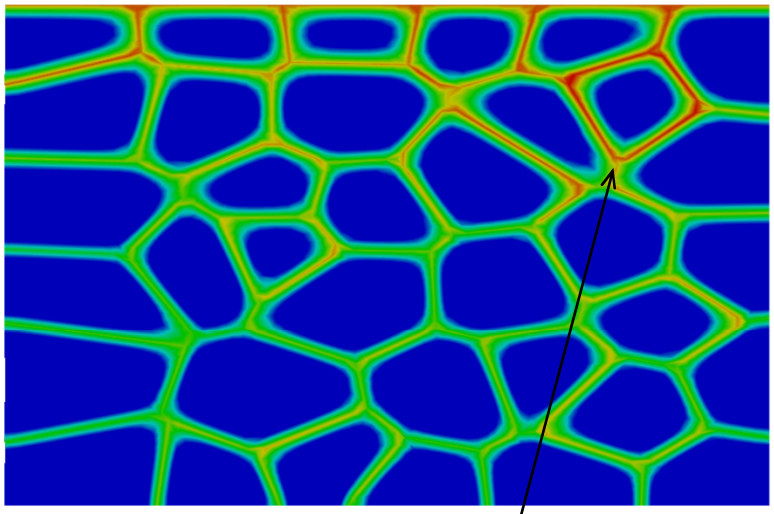

Diffusion speeds due to decreasing length

Solving 5 fields simultaneously

Units are scaled in the balance of linear momentum, conservation of concentration, and L_2 projection to improve condition number of the system

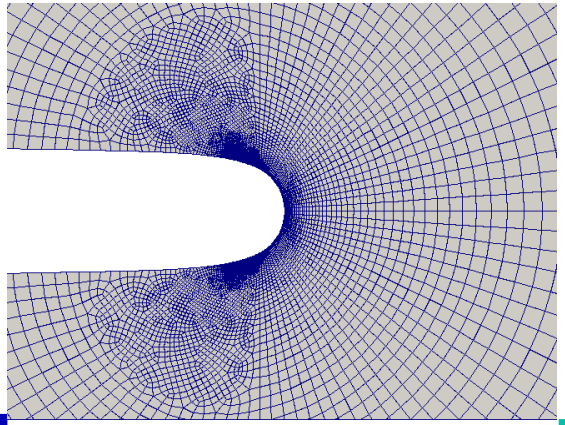

https://software.sandia.gov/albany/

$$D^* \dot{C}_L$$

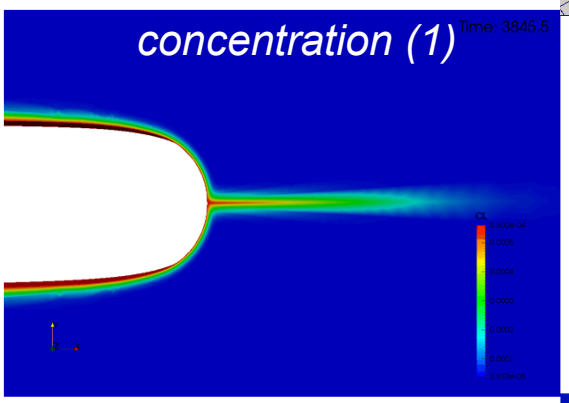

- Path: $10^5 D_0$
- K_{app}: 85 MPa $m^{1/2}$
- Time: 3850 s

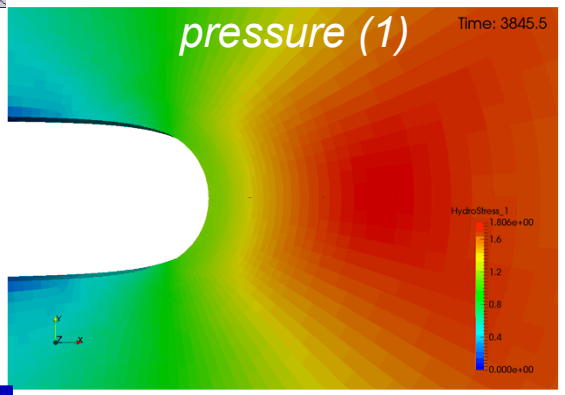

$$\nabla_{\boldsymbol{X}} \cdot d_l \boldsymbol{C}^{-1} \nabla_{\boldsymbol{X}} C_L$$

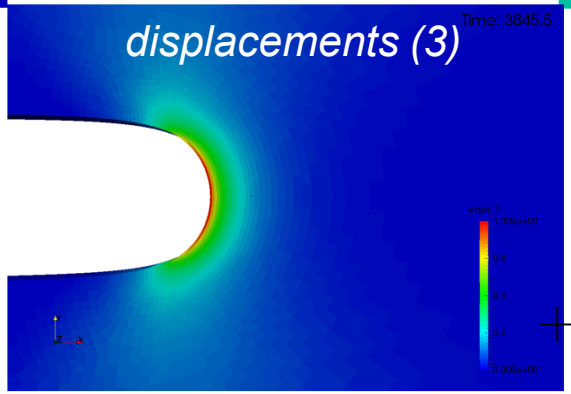

$$\nabla_{\boldsymbol{X}} \cdot \frac{d_l V_H}{RT} \boldsymbol{C}^{-1} \nabla_{\boldsymbol{X}} \tau_h C_L$$

$$+ \theta_T \frac{dN_T}{d\epsilon_p} \dot{\epsilon}_p$$

NOTE: 85 MPa $m^{1/2}$ is well below J_Q for 21Cr-6Ni-9Mn (220 MPa $m^{1/2}$)

Evolution of concentration at crack tip

Sandia National Laboratories

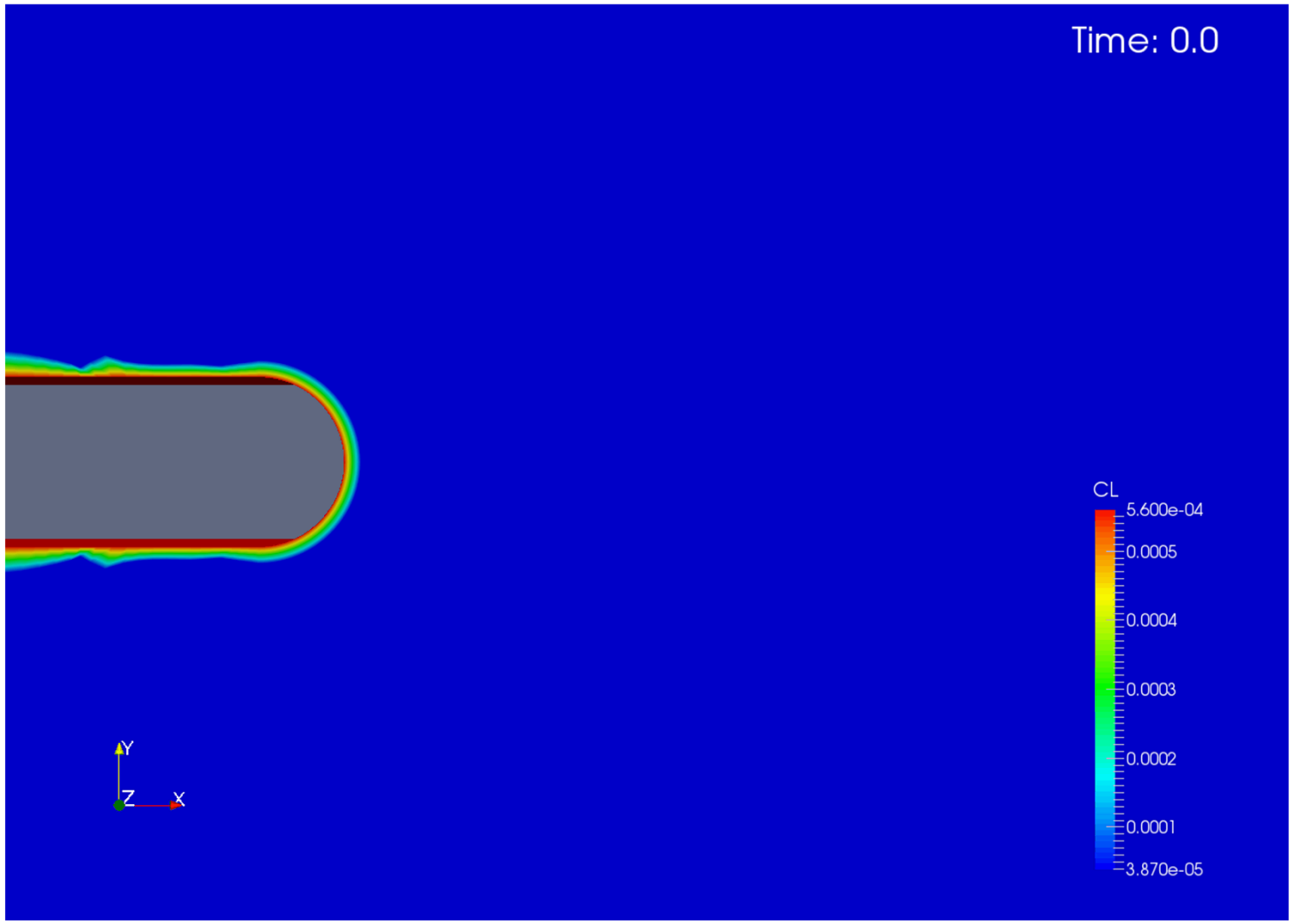

H isotope diffusion w/ He bubbles

We seek to find descriptors of helium bubble formation that result from the radioactive decay of tritium (T) to He.

- Schaldach and Wolfer (2004) focus on the total number of clusters (total bubble density)

1000s of ODEs for helium clusters are condensed into 3 coupled ODEs written in

- Single He (monomers) N_1, total bubble density, N_b, and bubble volume fraction S_b
- ODEs are nonlinear. We can integrate them implicitly with Newton's method
- Chemo-mechanical solution (T, **u**). Solve ODEs (dependent on T) at integration points.

$$\frac{dN_1}{dt} = G(t) - 16\pi(r_1 + r_1)DN_1^2 - 4\pi DN_1\left(\frac{3}{4\pi}\right)^{\frac{1}{3}} S_b^{\frac{1}{3}} N_b^{\frac{2}{3}}$$

$$\frac{dN_b}{dt} = 8\pi(r_1 + r_1)DN_1^2$$

$$\frac{\eta}{\Omega}\frac{dS_b}{dt} = 16\pi(r_1 + r_1)DN_1^2 + 4\pi DN_1\left(\frac{3}{4\pi}\right)^{\frac{1}{3}} S_b^{\frac{1}{3}} N_b^{\frac{2}{3}}$$

$$C_{He} = N_1 + \left(\frac{\eta}{\Omega}\right) S_b$$

G(t) – helium source term
r_1 - initial bubble radius
η - number of He atoms/vacant site
Ω - partial molar volume

Effects of tritium & helium on yield

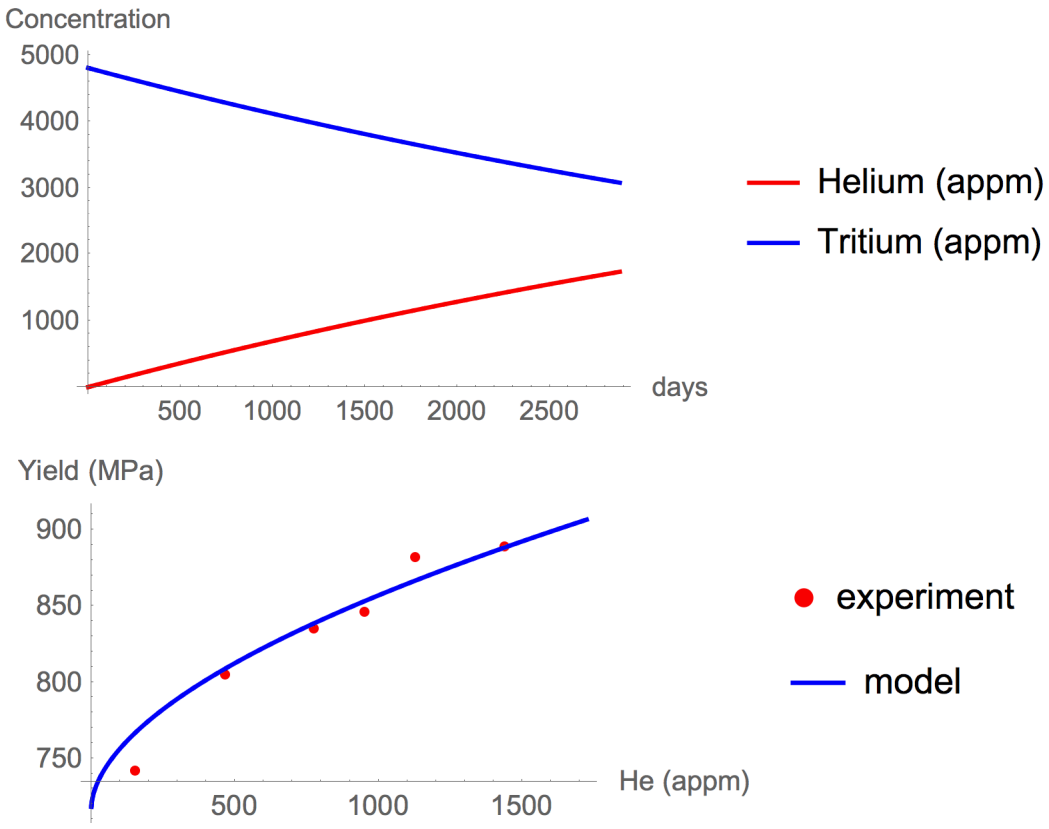

Comparison of current model to experimental data by Robinson and Thomas (1991). Data from hydrogen yields α_1 (hydrogen = tritium). Nonlinearity in fit stems from average bubble radius, not fitting parameter α_2. Both parameters are needed to accurately fit Robinson's data.

From helium bubble ODEs, we have:

N_b total bubble density

S_b bubble volume fraction

Calculate average bubble radius:

$$\bar{R}_b = \left(\frac{3 S_b}{4 \pi N_b} \right)^{\frac{1}{3}}$$

Assumptions for yield stress σ_y:

- Rate independent yield stress σ_0
- Proportional to T concentration, C_T
- Misfit strengthening from He is dominant (Arsenlis, Wolfer, JNM)
- Misfit strengthening varies w/R_b^2
- Normalize w/He atomic radius R_a

$$\sigma_y = \sigma_0 + \alpha_1 C_T + \alpha_2 \left(\frac{\bar{R}_b}{R_a} \right)^2$$

α_1 and α_2 are constants fit to experiments

Yield dominant in flow behavior

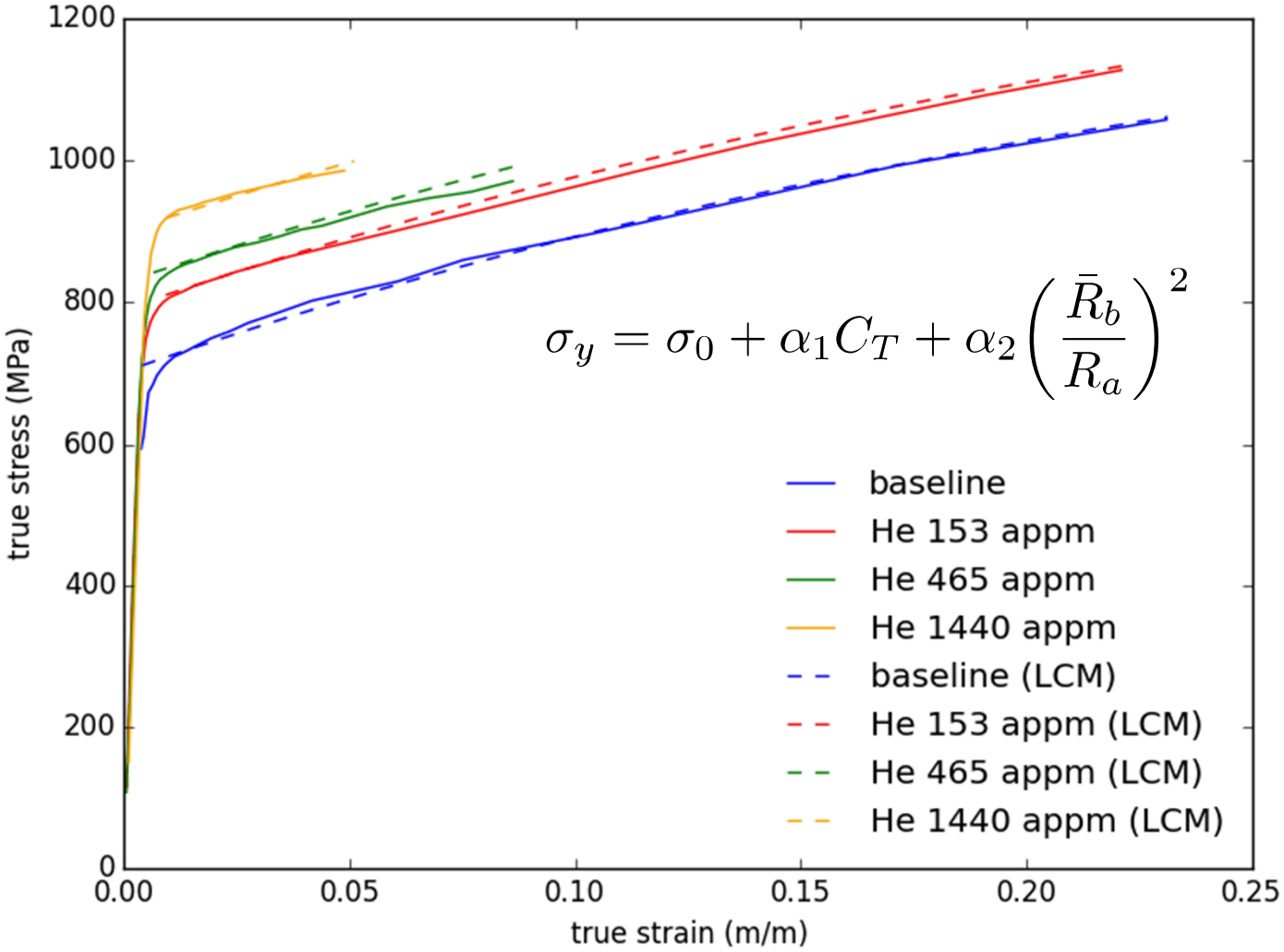

σ_0 = 710 MPa

H = 0.0149μ

R_d = 3.5

α_1 = 63.9 J/mol

α_2 = 4.1 MPa

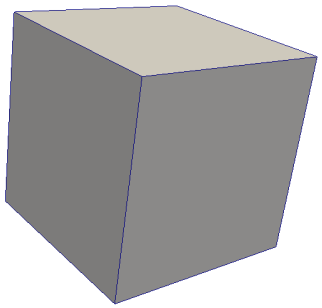

From Robinson and Thomas, "Accelerated Fracture due to Tritium and Helium in 21-6-9 Stainless Steel" (1991). *We cannot locate the source data. Missing He concentrations of 774, 950, and 1128 appm.*

T/He nucleation needed for failure

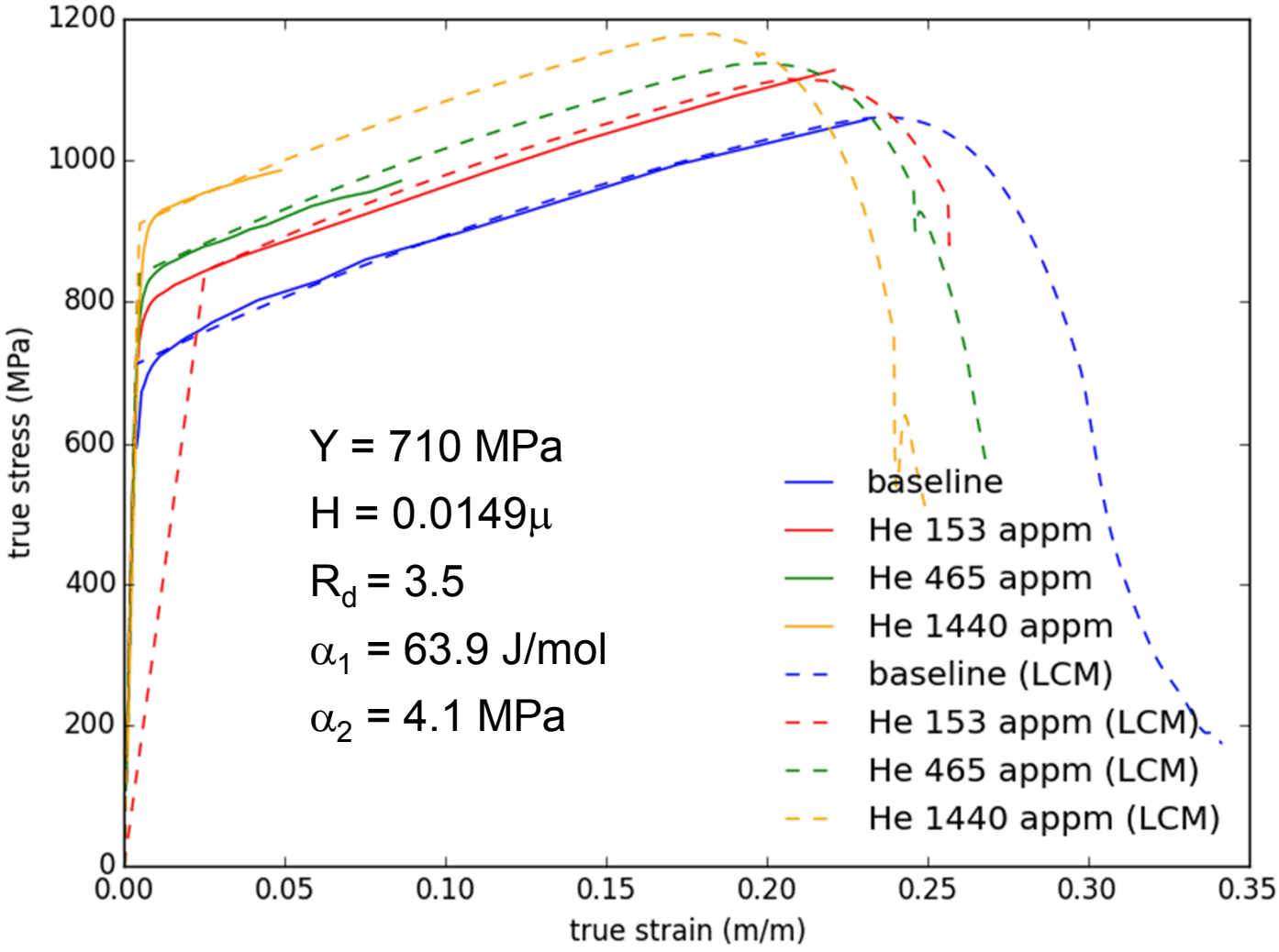

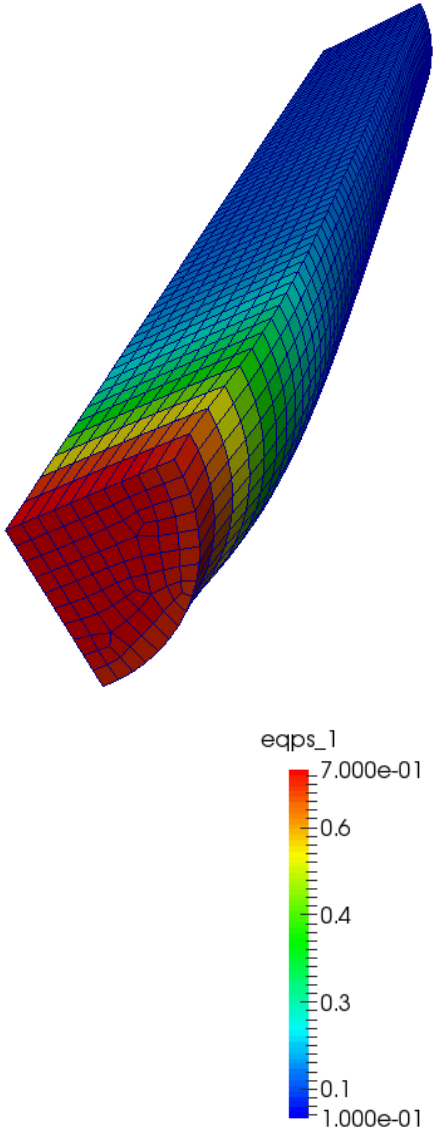

Model results reduced through volume preservation to create true stress-strain curves.

T/He nucleation, growth, coalescence

In spirit of Chu and Needleman (1980) we choose an appropriate state variable to capture void nucleation through elevated stresses at pile-ups.

void volume fraction for nucleation — mean ε_{ss} for nucleation

$$f_n(C_T, S_b) = \frac{\phi_{n,0}(S_b)}{\sqrt{2\pi}\sigma_{\epsilon_{ss}}} \exp\left[-\frac{1}{2}\left(\frac{\epsilon_{ss} - \mu_{\epsilon_{ss}}(C_T)}{\sigma_{\epsilon_{ss}}}\right)^2\right]$$

probability distribution — standard deviation

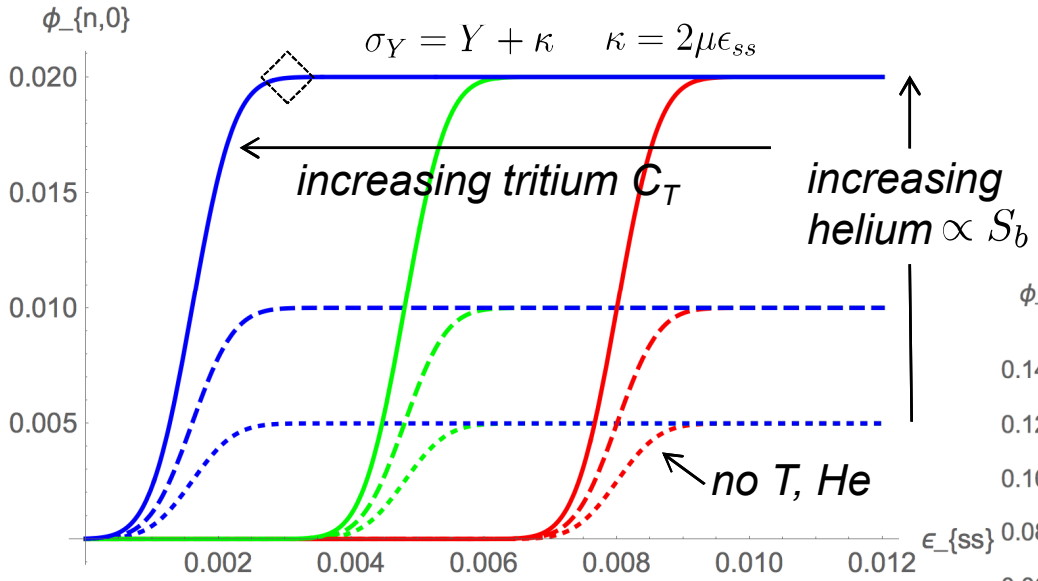

Statistical nucleation: Tritium localizes deformation and enables voids to nucleate earlier in the deformation. Helium-hardened microstructure nucleates more voids.

Initial model for void evolution:

- Void nucleation driven by deformation (dislocations, twins) $\propto \epsilon_{ss}$
  - Tritium C_T hastens process
  - Helium amplifies process
- Void growth through Gurson
- Void coalescence governed by S_b
  - Nucleated voids connected by smaller helium bubbles

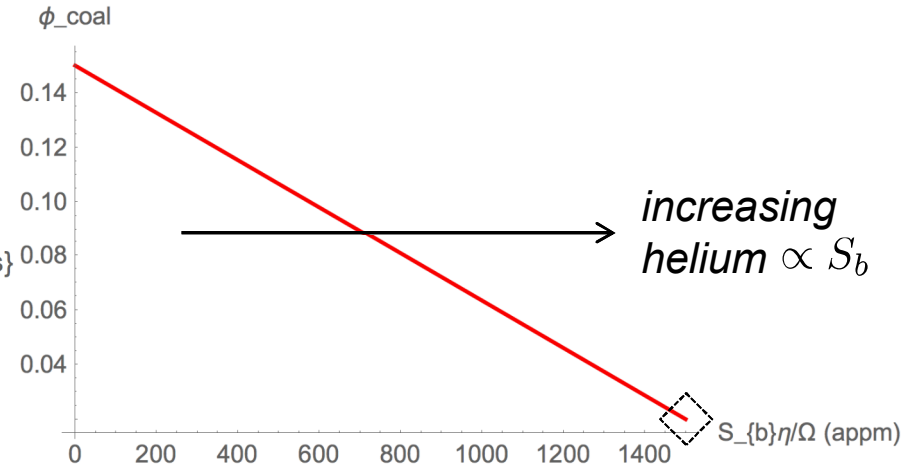

A tritium-embrittled, helium-hardened microstructure can move from nucleation to coalescence ◇

Crack initiation and growth in SFC

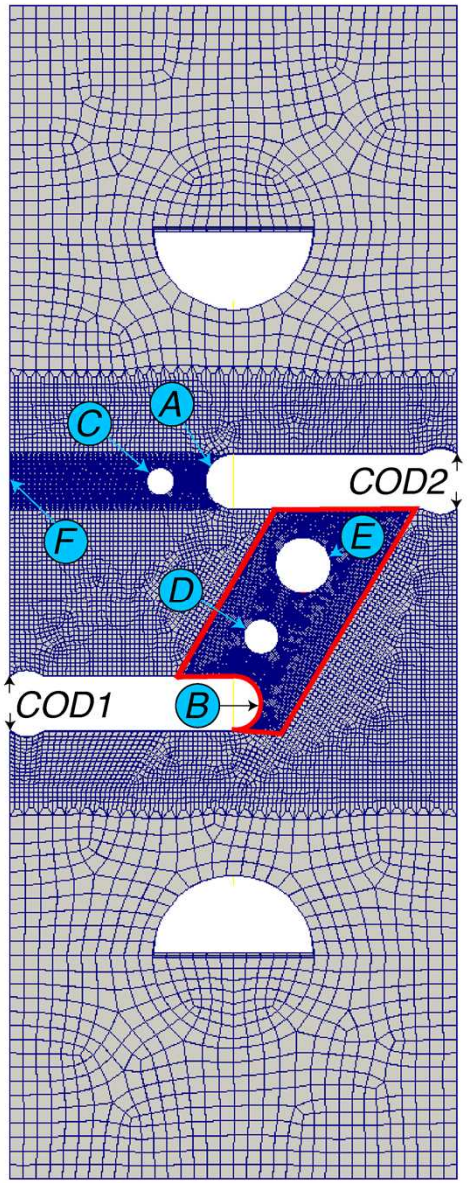

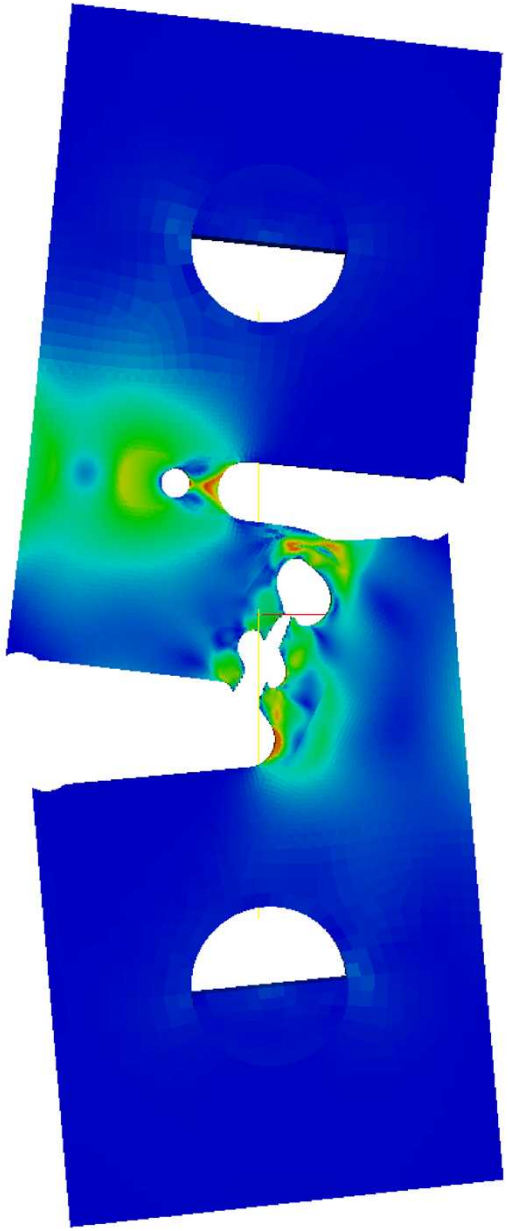

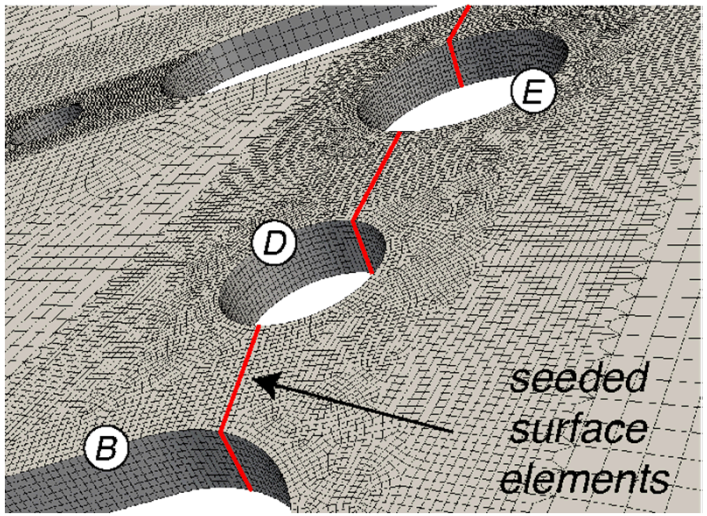

2nd Sandia Fracture Challenge (SFC)

- Ti-6Al-4V plate
- Anisotropy
- Mixed-mode loading
- Slow/fast rates of loading
- Thermomechanical coupling
- Dynamics (unstable propagation)
- Employed surface elements
- Multiple damage models
- Implicit solution
- *Sierra SolidMechanics*

Regularized solution

- Localization elements yield convergence in the load displacement curve at slow, isothermal rates
- Constitutive model incorporates anisotropy in yield and shear nucleation in damage evolution

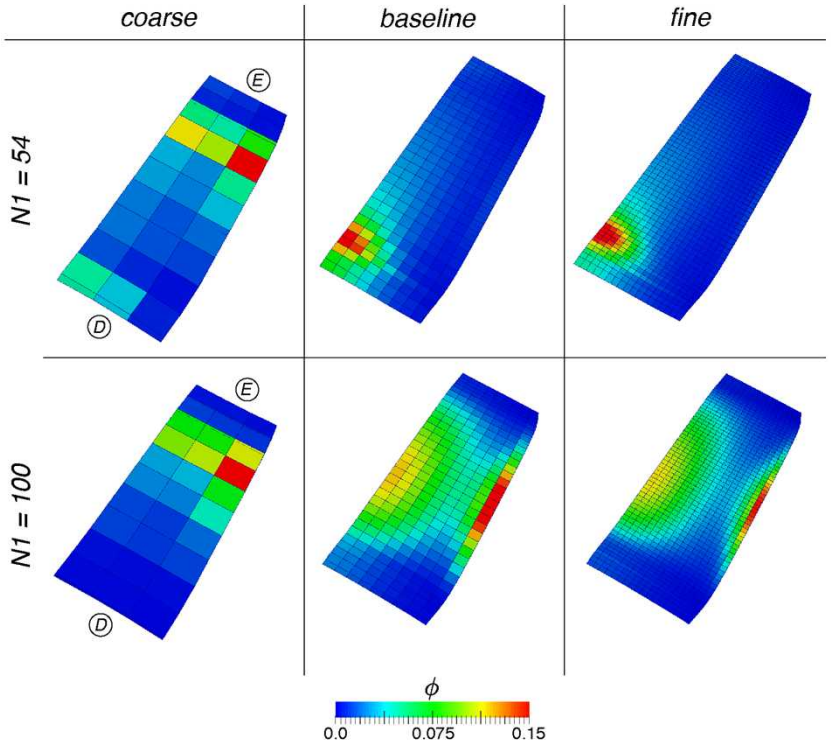

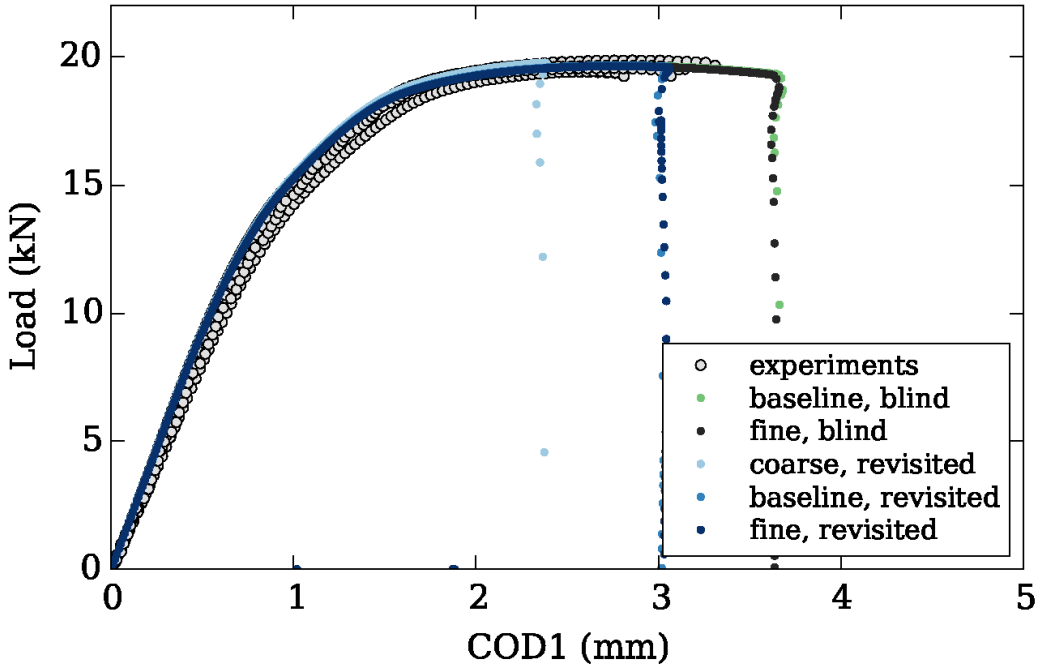

- Convergence in both the far-field and near-field quantities
- Increasing the role of shear nucleation (N1) transitions crack initiation from the interior to the surface

Summary and path forward

- Illustrated strong chemo-mechanical coupling
- Surface approaches capable of capturing multiphysics on multiple scales
- Progress in H/T/He embrittlement w/focus on void nucleation
- SFC illustrates the applicability of approach to H/T/He embrittlement
- Future work will focus on
  - Parameterization of nucleation processes and transition to coalescence
  - Predicting the time-dependent toughness of 21Cr-6-9Mn
  - Transitioning technology from research environment to production

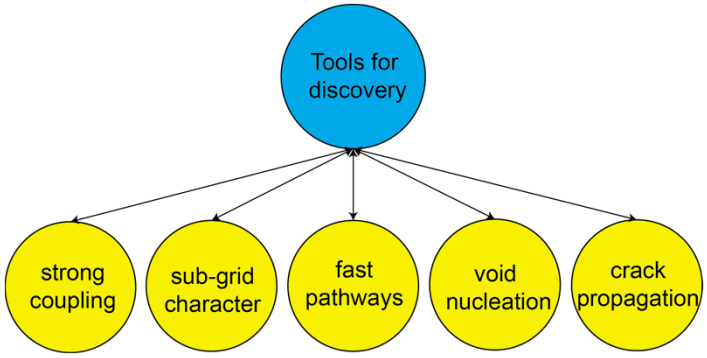

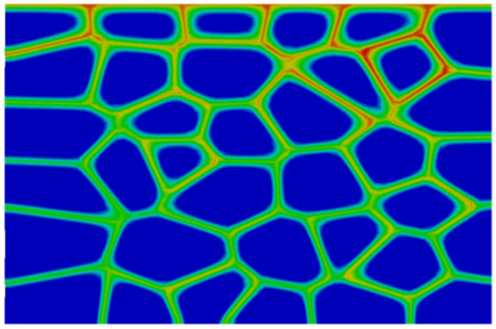

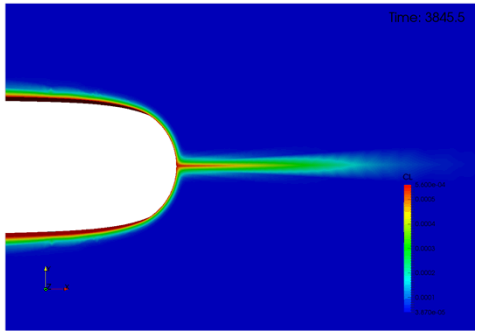

Sandia National Laboratories

BACKUP SLIDES

Damage nucleation model w/H

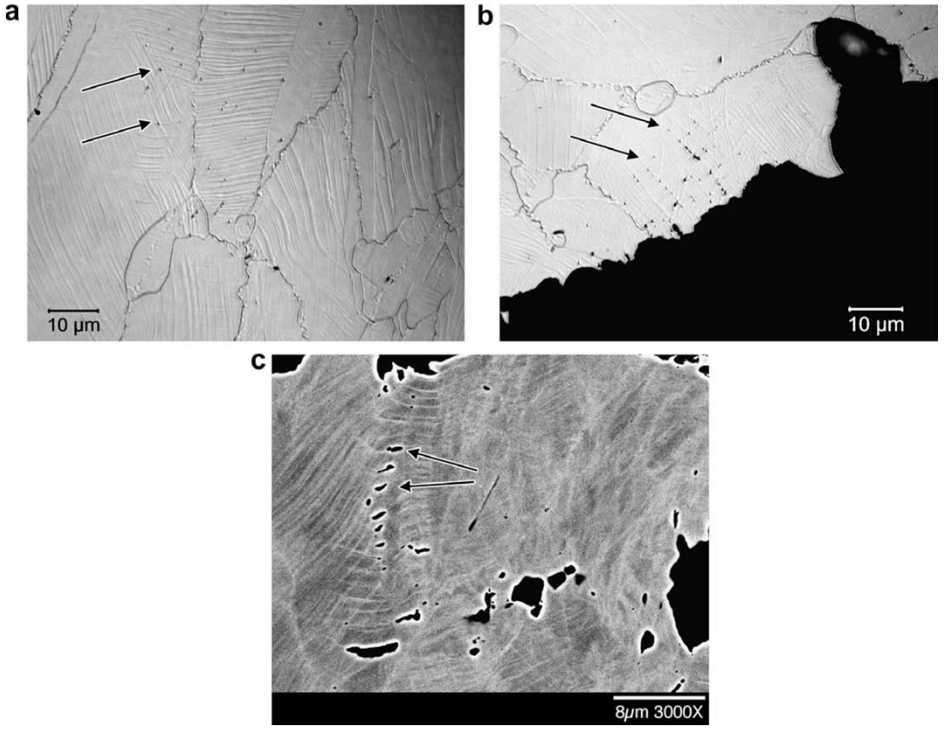

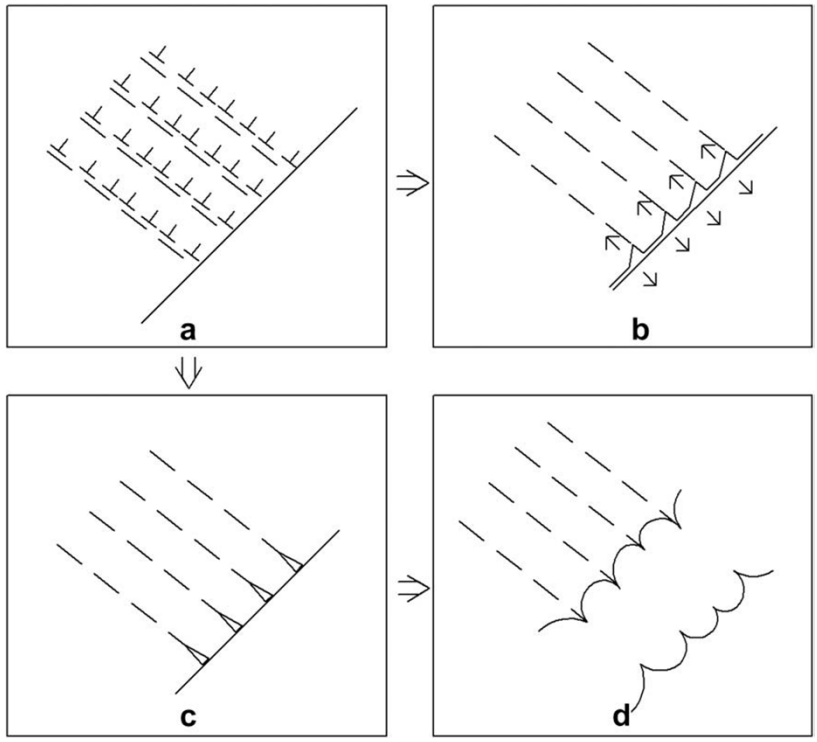

IDEA: Hydrogen enables the premature formation of planar deformation bands that impinge on boundaries of grains, annealing twins, and/or other deformation bands. The stress concentration induced by the intersection may nucleate a void of large aspect ratio (cylinder) that will evolve, coalesce and create the observed “fluted” fracture surface.

The fracture process is still ductile! Need to capture the premature nucleation of voids in the presence of hydrogen. Can we first construct a simple model to aid our intuition?

Analytical basis for nucleation

Stroh, A Theory of the Fracture of Metals, 1957

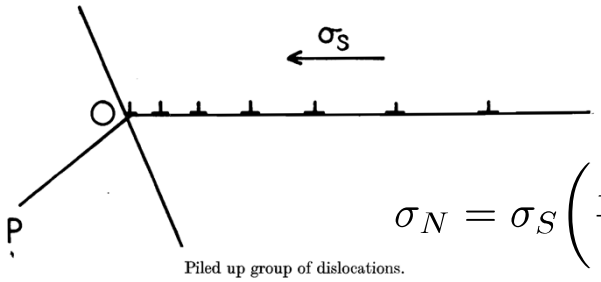

Piled up group of dislocations.

$$\sigma_N = \sigma_S \left(\frac{L}{r}\right)^{\frac{1}{2}} f(\theta)$$

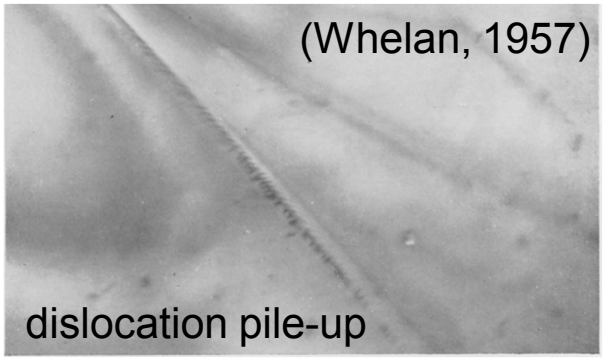

Using a work argument, the normal stress σ_N for nucleation can derived from the shear stress σ_S given the fracture energy γ and the number of dislocations *n* in a pile-up (band) along a boundary.

$$\sigma_{S,crit} = \frac{3\pi^2\gamma}{8n(\rho_{ss},\theta_T)b} \qquad n = A(\theta_T)\rho_{ss} = hs(\theta_T)\rho_{ss}$$

$$\kappa = \mu\epsilon_{ss}$$
$$\epsilon_{ss} = b\sqrt{\rho_{ss}}$$

Given *b* is burgers vector and *A* is an effective area characterized by the grain size *h* and the pile-up spacing *s*. We relate the pile-up spacing the to the occupancy of hydrogen in the traps θ_T. If we approximate σ_S through the yield stress σ_y and the isotropic hardening variable κ, we can express nucleation in terms of a scalar strain metric ε_{ss} that is reflective of the dislocation density ρ_{ss}.

$$\epsilon_{ss,crit}^3 + \frac{\sigma_y}{\mu}\epsilon_{ss,crit} - \frac{3\pi b\gamma}{4hs(\theta_T)\mu}$$

permits analytical solution (1 real root)

If we assume heavily worked materials, ρ_{ss} ~ 10^{15}, the specification of $s(\theta_T)$ becomes problematic. We need to construct a simplified model for nucleation in the correct state variable ε_{ss} that can capture a statistical sampling of boundary orientations having dislocation pile-ups (bands) which are stabilized and extended though hydrogen transport.

$$\theta_T = \frac{C_T}{N_T}$$

Occupancy of hydrogen in the traps θ_T derives from trapped concentration C_T and the number of traps N_T.

Phenomenological extension

The deformation bands that evolve under large deformations cannot be easily idealized

$$f_n = \frac{\phi_{n,0}}{\epsilon_{ss,std}\sqrt{2\pi}} \exp\left[-\frac{1}{2}\left(\frac{\epsilon_{ss}-\epsilon_{ss,mean}}{\epsilon_{ss,std}}\right)^2\right]$$

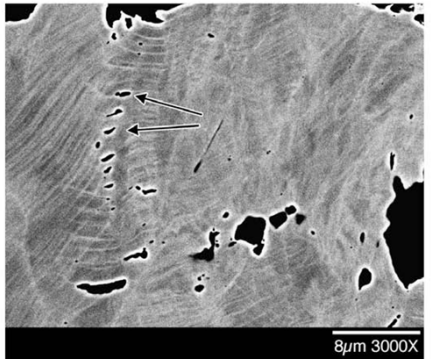

(Nibur, 2009)

In spirit of Chu and Needleman (1980) we choose an appropriate state variable to capture void nucleation through elevated stresses at pile-ups. We assume the probability of void nucleation f_n follows a normal distribution.

We assume that hydrogen affects the mean $\varepsilon_{ss,mean}$ and not the standard deviation $\varepsilon_{ss,std}$ through the occupancy of hydrogen in the traps θ_T. The nucleated void volume fraction ϕ_n can be found through integration and is limited by $\phi_{n,0}$.

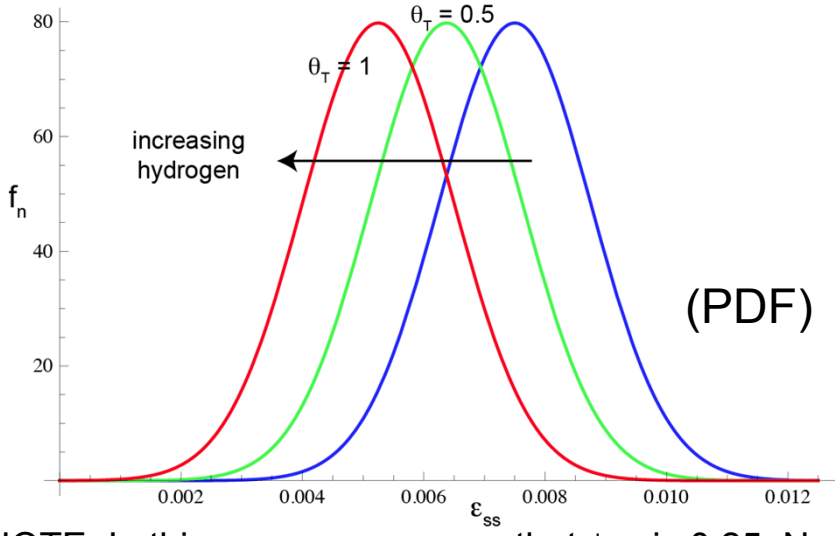

(PDF)

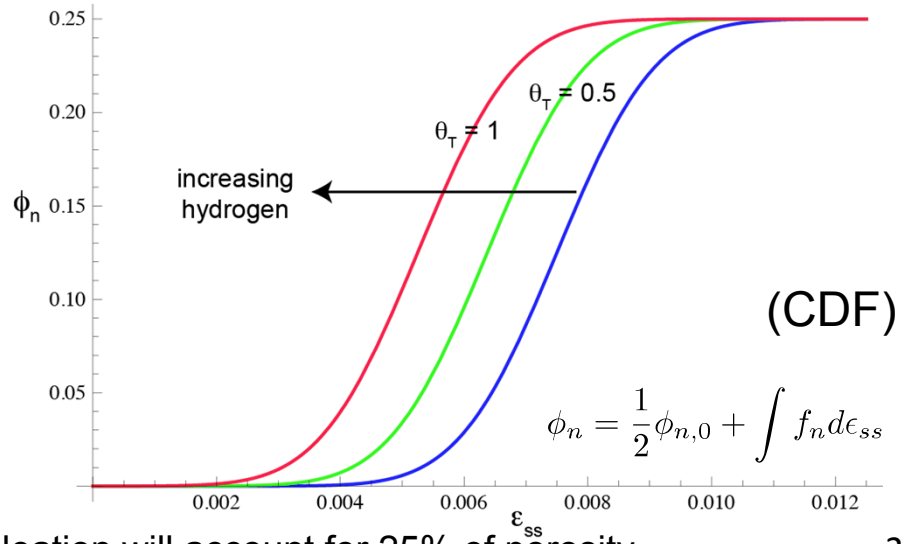

(CDF)

$$\phi_n = \frac{1}{2}\phi_{n,0} + \int f_n d\epsilon_{ss}$$

NOTE: In this case, we assume that $\phi_{n,0}$ is 0.25. Nucleation will account for 25% of porosity

Modeling 21Cr-6Ni-9Mn in H_2 gas

Before moving to complex and computationally challenging fracture geometries, we need to understand phenomena in plane strain

Mechanical analysis should be performed to help experimentalists reduce driving forces from non-standard fracture geometry. Iteration required.

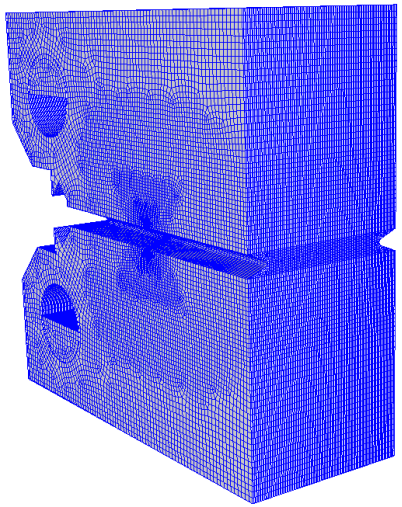

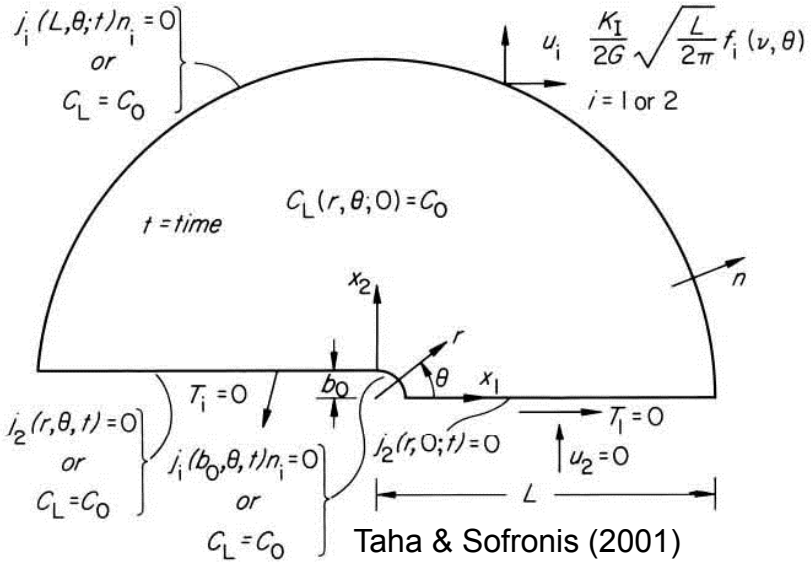

Taha & Sofronis (2001)

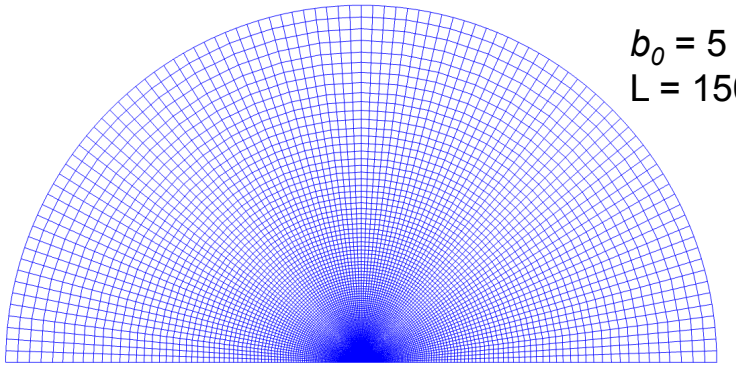

b_0 = 5 μm
L = 150 mm

nodes: 189,312
h: 40 nm x 200 nm

NOTE: Not pre-charged, constant concentration $C_{L,applied}$ applied to crack faces

Coupled hydrogen transport

Sandia National Laboratories

This path heavily leverages Sofronis/McMeeking (1989)* and Krom (1998). Recent work by Leo and Anand (2013).

chemical potential

$$\mu_l = \mu_0 + RT\ln(\theta_l) - v_h\sigma_h$$

$$\boldsymbol{F} = \frac{\partial \boldsymbol{x}}{\partial \boldsymbol{X}} \qquad J = \det[\boldsymbol{F}]$$

$$\theta_l = c_l/n_l \qquad \theta_t = c_t/n_t$$

$$n_l = N_L/J \qquad n_t = N_T(\epsilon_p)/J$$

$$v_h = V_H J \qquad \tau_h = J\sigma_h$$

$$\boldsymbol{d}_l = RT\boldsymbol{m}_l$$

model for flux

$$\boldsymbol{j}_l = -\boldsymbol{m}_l c_l \nabla_{\boldsymbol{x}}\mu_l$$

conservation of hydrogen

$$\frac{d}{dt}\int_B c dv = -\int_{\partial B} \boldsymbol{j}\cdot\boldsymbol{n} da \qquad \dot{c} = \dot{c}_l + \frac{\partial c_t}{\partial cl}\dot{c}_l + \frac{\partial c_t}{\partial n_t}\frac{\partial n_t}{\partial \epsilon_p}\dot{\epsilon}_p + \frac{\partial c_t}{\partial n_t}\frac{\partial n_t}{\partial J}\dot{J}$$

$$c_t = c_t(c_l, \epsilon_p, J)$$

equilibrium of lattice/trap sites

$$\theta_t = \frac{1}{1+\frac{1}{k_t\theta_l}} \qquad C^* = c_l + \frac{n_t}{1+\frac{n_l}{k_t c_l}} \qquad D^* = 1 + \frac{\partial c_t}{\partial c_l}$$

$$D^*\dot{c}_l + C^*\mathrm{div}\boldsymbol{v} - \nabla_{\boldsymbol{x}}\cdot\boldsymbol{d}_l\nabla_{\boldsymbol{x}}c_l - \nabla_{\boldsymbol{x}}\cdot\frac{c_l}{J}\boldsymbol{d}_l\nabla_{\boldsymbol{x}}J + \nabla_{\boldsymbol{x}}\cdot\frac{c_l V_H}{RT}\boldsymbol{d}_l\nabla_{\boldsymbol{x}}\tau_h +$$

$$\frac{\theta_l}{J}\frac{\partial N_T}{\partial \epsilon_p}\dot{\epsilon}_p - \frac{\theta_t N_T}{J^2}\dot{J} = 0$$

*P. Sofronis and R.M. McMeeking, J. Mech. Phys. Solids 37 (1989) 317

Baseline properties for 21Cr-6Ni-9Mn

*Transport**

D_0 = 5.4E-7 m^2/s
Q = 53.9E3 J/mol
R = 8.314 J/(mol K)
T = 300 K
D_L = 2.2E-16 m^2/s
N_A = 6.0232 atoms/mol
V_M = 7.116E-6 m^3/mol – molar volume of Fe
V_H = 2.0E-6 m^3/mol – partial molar volume of H
N_L = 8.46E28 atoms/m^3 = 1.40E5 solvent lattice mol/m^3
$C_{L,0}$ = 38.7 mol/m^3 (from 316 alloys, assumes 5 wppm)
$C_{L,applied}$ = 560 mol H/m^3 (280 moles H_2/m^3)
$N_{T,total} = \alpha N_T = 10N_T = 10^{(26.6 - 1.5\exp(-6.96ep))}$ mole/m^3
$C_{T,0}$ = 3.94E24 atoms/m^3 = 6.542 mol/m^3
W_B = 9.65E3 J/mol
K_T = 47.9

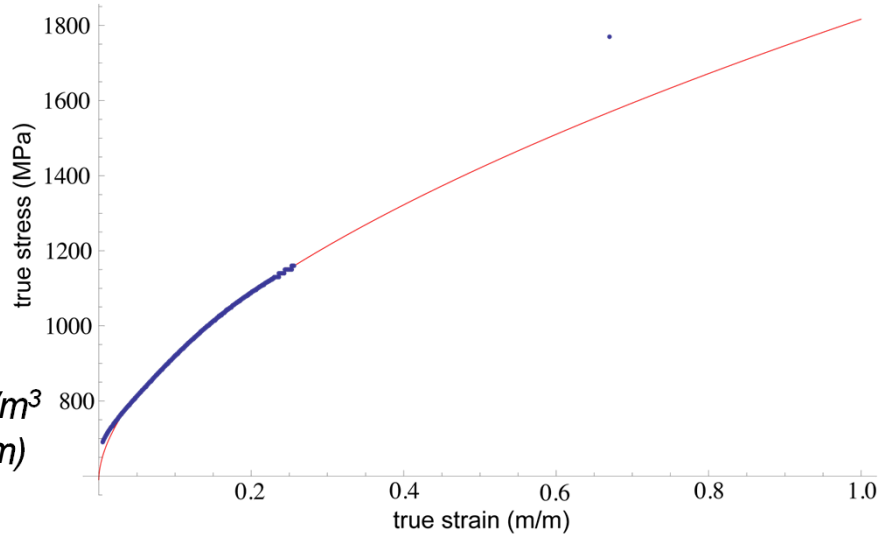

$C_{L,applied} = Kf^{\frac{1}{2}}$ San Marchi, et al., IJHE, 2007

Mechanics – non-charged, forged, transverse, LF

ρ = 7806 kg/m^3
E = 196.6 GPa
ν= 0.3
σ_0 = 590 MPa
H = 1227 MPa
m = 0.563

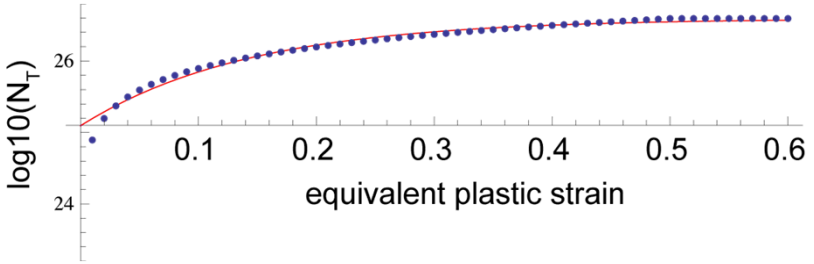

*Transport properties aligned with Somerday, et al., Met Trans, 2009

NOTE: Constant concentration, not chemical potential, is applied. Will fix.

Initial studies in 21Cr-6Ni-9Mn SS

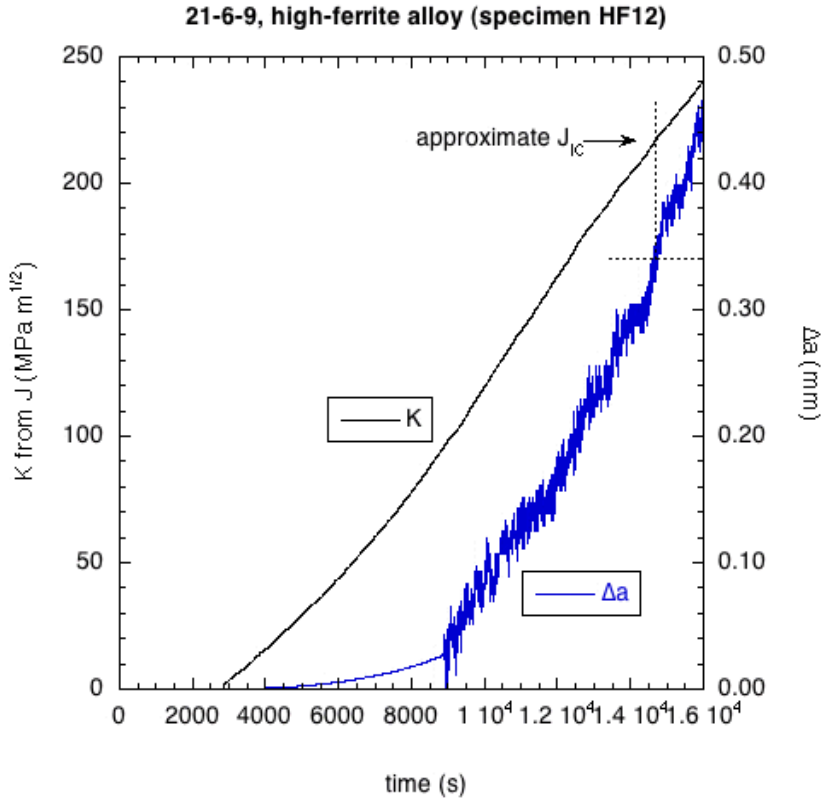

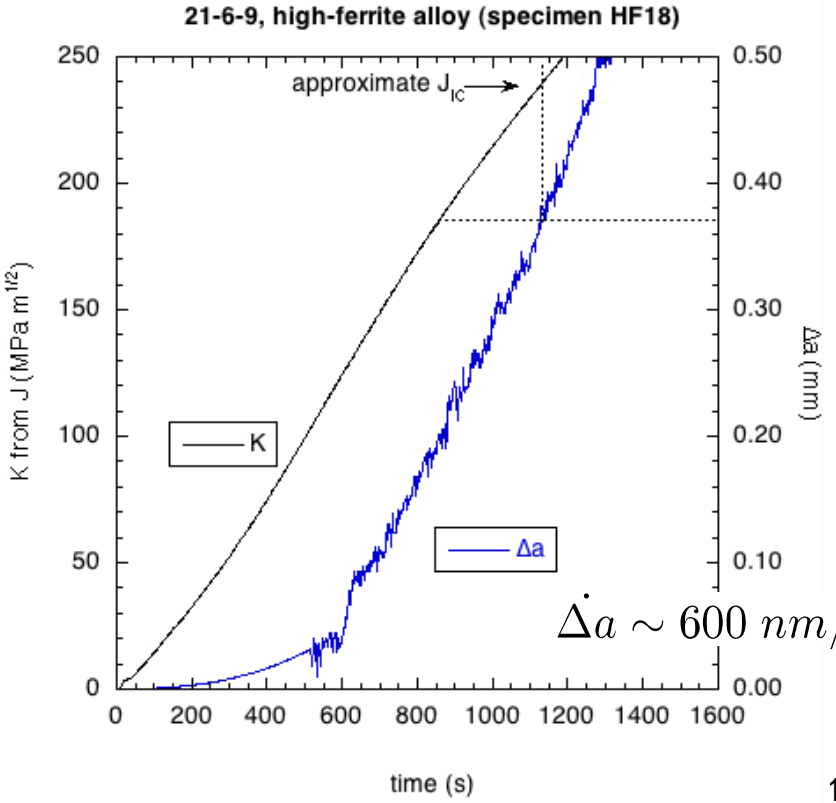

$\dot{\Delta a} \sim 600\ nm/s$

18)